

Color-tunable upconversion luminescence of Yb³⁺, Er³⁺, and Tm³⁺ tri-doped ferroelectric BaTiO₃ materials

Yang Zhang and Jianhua Hao

Citation: *J. Appl. Phys.* **113**, 184112 (2013); doi: 10.1063/1.4805050

View online: <http://dx.doi.org/10.1063/1.4805050>

View Table of Contents: <http://jap.aip.org/resource/1/JAPIAU/v113/i18>

Published by the AIP Publishing LLC.

Additional information on J. Appl. Phys.

Journal Homepage: <http://jap.aip.org/>

Journal Information: http://jap.aip.org/about/about_the_journal

Top downloads: http://jap.aip.org/features/most_downloaded

Information for Authors: <http://jap.aip.org/authors>

ADVERTISEMENT



AIP Advances

Now Indexed in Thomson Reuters Databases

Explore AIP's open access journal:

- Rapid publication
- Article-level metrics
- Post-publication rating and commenting

Color-tunable upconversion luminescence of Yb³⁺, Er³⁺, and Tm³⁺ tri-doped ferroelectric BaTiO₃ materials

Yang Zhang^{1,2} and Jianhua Hao^{1,2,a)}

¹The Hong Kong Polytechnic University, Shenzhen Research Institute, Shenzhen 518057, People's Republic of China

²Department of Applied Physics, The Hong Kong Polytechnic University, Hong Kong, People's Republic of China

(Received 12 February 2013; accepted 29 April 2013; published online 14 May 2013)

Tunable upconversion (UC) multicolor luminescence is observed from Yb³⁺, Er³⁺, and Tm³⁺ tri-doped ferroelectric BaTiO₃ (BTO) materials. By control of dopant concentrations, the lanthanide-doped BTO powders are capable of generating various UC spectra and color tunability. A white-light emission is achieved through an optimal design. Strong UC luminescence is also observed in the lanthanide-doped BTO thin-films grown on Pt/TiO₂/SiO₂/Si substrate, which can retain well-defined hysteresis loops with a remnant polarization (2P_r) of 17.8 μC/cm². These findings open the possibility of lanthanide-doped BTO as multifunctional materials, in which both luminescent and ferroelectric properties co-exist. © 2013 AIP Publishing LLC. [<http://dx.doi.org/10.1063/1.4805050>]

I. INTRODUCTION

Near infrared to visible upconversion (UC) luminescence in lanthanide (Ln³⁺)-doped materials has shown great applications in light-emitting display, lasers, biological labeling, and optoelectronic devices.¹⁻⁴ In recent years, much interest has been focused on multicolor tunability of UC emission to meet the requirements of these applications. Owing to their abundant ladder-like energy levels, trivalent lanthanide ions, such as Er³⁺, Tm³⁺, Eu³⁺, and Pr³⁺, have been extensively studied as activator ions for UC processes.⁵ Up to now, several trivalent lanthanide-doped UC materials have demonstrated that the tuning of UC multicolor can cover the whole visible light region by adjusting relative intensity of three primary colors red-green-blue (RGB).⁶ In particular, by precise control of the combination and concentration of Ln³⁺ ions, one may obtain efficient and single-phased white-light emitting phosphors.^{7,8} To date, many researchers have developed several types of UC color-tunable phosphors based on various host matrices (such as rare-earth oxides, rare-earth fluorides, alkaline earth metal fluorides, and so on),⁹⁻¹² doped with suitable Ln³⁺ ions that have found vital applications in different fields. However, there is limited investigation on the UC emission and color tunability in ferroelectric materials.

Ferroelectric titanates, such as BaTiO₃ (BTO) with perovskite ABO₃ structure, have been involved in many important technical applications due to their excellent dielectric, ferroelectric, and electro-optic properties.^{13,14} These highly functional perovskite-type oxides are also recognized to be an important class of host matrices for Ln³⁺ ions due to their important properties, such as chemical and mechanical stability, as well as low vibrational frequency which makes them suitable as UC phosphor host matrices.^{15,16} In addition,

BTO based ferroelectric materials have shown large electro-optic coefficient and high photorefractive sensitivity which is of great benefit to photonic application.¹⁷ We have previously observed that the temperature dependence of UC emission in Er³⁺-doped BTO powders is associated with phase transitions of BTO host.¹⁸ Recently, we have presented an approach to enhance and modulate UC emission through applying a relatively low bias voltage to the Ln³⁺-doped BTO thin film.¹⁹ The realization of UC emission in Ln³⁺-doped ferroelectric materials provides us an opportunity to develop a class of “smart” materials with luminescence properties that change in response to external stimuli including electric field, mechanical force, temperature, and so on.

In this work, we report the color-tunable UC luminescence of ferroelectric BTO doped with Yb³⁺, Er³⁺, and/or Tm³⁺ ions via solid-state reaction method. Tunable UC multicolor emissions including white color are obtained. Furthermore, with the exploitation and application of the thin-film luminescent devices, it becomes more important to investigate the relative properties of integrated optical system compatible with semiconductor wafer. Herein, strong UC luminescence is observed in Ln³⁺-doped BTO thin-films grown on Pt/TiO₂/SiO₂/Si (Pt-Si) substrates. Meanwhile, the studies of ferroelectric properties of the thin-film structure are also presented.

II. EXPERIMENTAL

Yb³⁺/Er³⁺/Tm³⁺ tri-doped BTO powders were synthesized by conventional solid-state reaction method. Reagent grade BaCO₃, TiO₂, Yb₂O₃, Er₂O₃, and Tm₂O₃ powders were used as raw materials. Yb³⁺, Er³⁺, and Tm³⁺ were substituted at the Ti⁴⁺ site; the negative effective charge can be compensated by oxygen vacancy. Thus, the formula is given by BaTi_{1-x-y-z}Yb_xEr_yTm_zO_{3-δ} (BTO:xYb³⁺, yEr³⁺, zTm³⁺, in which x, y, and z are the doping concentrations in molar percentage). Based on the above formula, the starting powders

^{a)}Author to whom correspondence should be addressed. Electronic mail: jh.hao@polyu.edu.hk.

were weighted with designed stoichiometric quantities and ball milled for 24 h, then dried and calcinated at 1100 °C for 8 h in air to prepare the powders. The resulting powders were pressed into disk pellets and sintered at 1350 °C for 4 h in air. The as-prepared target was used for depositing $\text{Yb}^{3+}/\text{Er}^{3+}/\text{Tm}^{3+}$ tri-doped BTO (BTO:Yb/Er/Tm) thin films. The BTO:Yb/Er/Tm films were grown on (100)-oriented Si wafer with a (111)-oriented Pt buffered layer by pulsed laser deposition (PLD). The BTO:Yb/Er/Tm films were deposited with the substrate temperature of 680 °C and oxygen pressure of 20 Pa. An ITO layer as a top transparent electrode was deposited on the BTO:Yb/Er/Tm film at 250 °C under 2.5 Pa oxygen ambient by PLD.

The crystal structures of the Ln^{3+} -doped BTO powders and thin films were examined by a Bruker D8 Advance X-ray diffractometer and a Bruker D8 Discover X-ray diffractometer with Cu K α radiation, respectively. The surface morphology of the films was investigated by field-emission scanning electron microscopy (FE-SEM, JEOL-JSM 6335 F). The photoluminescence (PL) spectra were recorded using an Edinburgh FLSP920 spectrophotometer under the excitation of a 980 nm laser diode. The hysteresis curves of the films were measured by the TF Analyzer 2000 on FE mode. The ferroelectric loops were recorded using a triangular wave form at a frequency of 1 kHz. All measurements were carried out at room temperature.

III. RESULTS AND DISCUSSION

Figure 1 shows the XRD patterns of BTO: Ln^{3+} ($\text{Ln}^{3+} = \text{Yb}^{3+}, \text{Er}^{3+}$ and Tm^{3+}) with different combinations and concentrations. Only the characteristic diffraction peaks of tetragonal BTO phase without secondary impurity phases can be observed, suggesting that $\text{Yb}^{3+}, \text{Er}^{3+}$, and Tm^{3+} ions were doped efficiently into the BTO host lattice. Our XRD results are in correlation with JCPDS card No. 89-1428. In addition, Ln^{3+} ions have larger radii than that of Ti^{4+} ion. As can be seen in the inset of Fig. 1, when the Ti^{4+} ions are substituted by Ln^{3+} ions, compared with pure BTO, the diffraction peak (111) of the as-obtained BTO powders show a minor shift

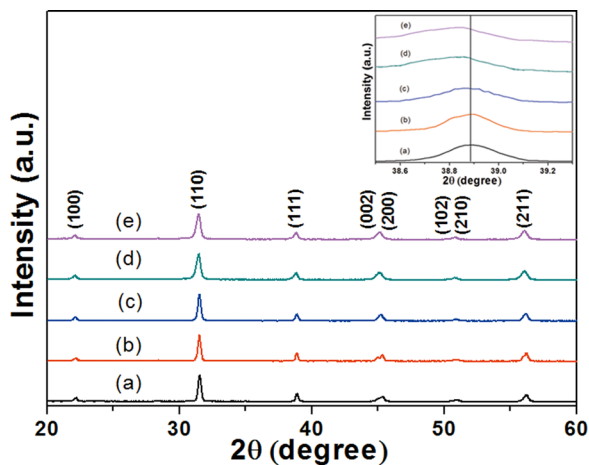


FIG. 1. XRD patterns of BTO: $x\text{Yb}^{3+}, y\text{Er}^{3+}, z\text{Tm}^{3+}$ powders: (a) pure BTO, (b) BTO:2% $\text{Yb}^{3+}, 0.2\%\text{Tm}^{3+}$; (c) BTO:2% $\text{Yb}^{3+}, 0.1\%\text{Er}^{3+}, 0.2\%\text{Tm}^{3+}$; (d) BTO:5% $\text{Yb}^{3+}, 0.1\%\text{Er}^{3+}, 0.2\%\text{Tm}^{3+}$; and (e) BTO:5% $\text{Yb}^{3+}, 0.2\%\text{Er}^{3+}, 0.2\%\text{Tm}^{3+}$. The inset shows the enlarged (111) peak.

towards low diffraction angle. It means that the lattice constant of Ln^{3+} -doped BTO expands compared with undoped BTO. These results are consistent with previous studies.^{18,20}

Figure 2 displays the UC luminescence spectra of BTO: Ln^{3+} phosphors doped with (a) 2% $\text{Yb}^{3+}, 0.2\%\text{Tm}^{3+}$; (b) 2% $\text{Yb}^{3+}, 0.1\%\text{Er}^{3+}$, and 0.2% Tm^{3+} ; (c) 5% $\text{Yb}^{3+}, 0.1\%\text{Er}^{3+}$, and 0.2% Tm^{3+} ; (d) 5% $\text{Yb}^{3+}, 0.02\%\text{Er}^{3+}, 0.2\%\text{Tm}^{3+}$, respectively. Figure 2(a) shows the UC emission spectrum of the BTO:2% $\text{Yb}^{3+}, 0.2\%\text{Tm}^{3+}$ sample. The blue emissions centered at about 464 and 478 nm can be attributed to the $^1\text{D}_2 \rightarrow ^3\text{F}_4$ and $^1\text{G}_4 \rightarrow ^3\text{H}_6$ transitions of Tm^{3+} ion, respectively. The red emissions appeared in the region (630–710 nm) consists of two bands located at 650 and 695 nm corresponding to $^1\text{G}_4 \rightarrow ^3\text{F}_4$ and $^3\text{F}_2/3\text{F}_3 \rightarrow ^3\text{H}_6$ transitions, respectively. To demonstrate the strong effect of dopant concentrations on multicolor emission, Er^{3+} ions were co-doped into the BTO host lattice. As can be seen in Figure 2(b), an intense green emission band located at 523 and 552 nm and a minor red emission band centered at 656 nm are observed, which are ascribed to $^2\text{H}_{11/2}/^4\text{S}_{3/2} \rightarrow ^4\text{I}_{15/2}$ and $^4\text{F}_{9/2} \rightarrow ^4\text{I}_{15/2}$ transitions of Er^{3+} ion, respectively.

For better understanding of the UC processes, Figure 3 shows the energy level diagrams of the $\text{Yb}^{3+}, \text{Er}^{3+}$, and Tm^{3+} ions, as well as the proposed UC mechanism under 980 nm laser excitation.¹⁹ Since the Yb^{3+} concentration is very high with respect to that of Er^{3+} and Tm^{3+} , the most possible UC processes is the energy transfer occurring from the Yb^{3+} ions to the Er^{3+} and Tm^{3+} ions. As can be seen in Fig. 3, the strong blue emission at 476 nm is clearly a three-step and three-photon process. High Yb^{3+} concentration may contribute to an increase in energy transfer efficiency between Yb^{3+} and Tm^{3+} ions, resulting in an enhanced blue emission of the Tm^{3+} ions (Fig. 2(c)). Upon increasing Yb^{3+} concentration, the ratio of green to the red emission also decreases. The higher Yb^{3+} concentration could enhance the red UC emission by quenching the $^4\text{S}_{3/2}$ level to the $^4\text{I}_{13/2}$ level of Er^{3+} ion through the so-called energy back-transfer process, i.e., $^4\text{S}_{3/2} (\text{Er}^{3+}) + ^2\text{F}_{7/2} (\text{Yb}^{3+}) \rightarrow ^4\text{I}_{13/2} (\text{Er}^{3+}) + ^2\text{F}_{5/2} (\text{Yb}^{3+})$ as shown in Fig. 3.²¹ The Er^{3+} ion at $^4\text{I}_{13/2}$ level

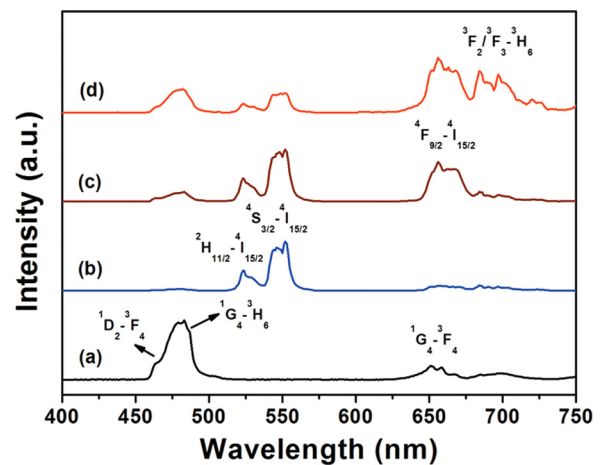


FIG. 2. UC emission spectra of BTO: Ln^{3+} phosphors under 980 nm laser excitation. (a) BTO:2% $\text{Yb}^{3+}, 0.2\%\text{Tm}^{3+}$; (b) BTO:2% $\text{Yb}^{3+}, 0.1\%\text{Er}^{3+}, 0.2\%\text{Tm}^{3+}$; (c) BTO:5% $\text{Yb}^{3+}, 0.1\%\text{Er}^{3+}, 0.2\%\text{Tm}^{3+}$; and (d) BTO:5% $\text{Yb}^{3+}, 0.02\%\text{Er}^{3+}, 0.2\%\text{Tm}^{3+}$.

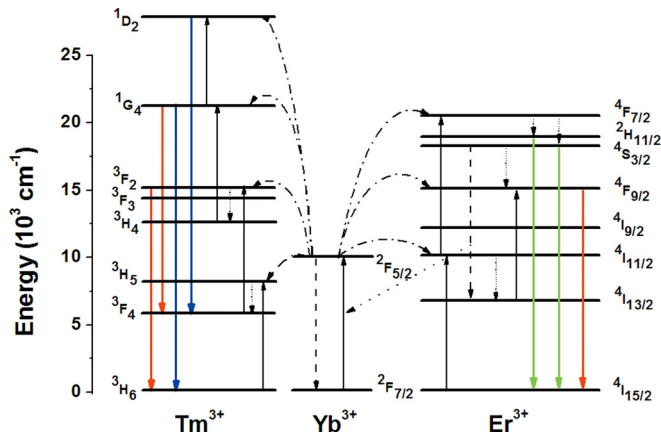


FIG. 3. Energy level diagram of Yb^{3+} , Er^{3+} , and Tm^{3+} , as well as the proposed UC mechanisms under 980 nm laser excitation.

subsequently absorbs one photon and jumps to the $^4\text{F}_{9/2}$ level, thus the enhanced population of the $^4\text{F}_{9/2}$ state is of benefit of the red UC emission. It indicates that the emission colors can be easily tuned by adjusting the concentration of Yb^{3+} ion.

Therefore, we have presented a versatile approach to tuning emission colors by control of dopant combinations and concentrations. Accordingly, a series of Ln^{3+} -doped BTO with different compositions are synthesized. The chromaticity coordinates (x , y) of the as-synthesized $\text{BTO}:\text{Ln}^{3+}$ are summarized in Table I. The variation of UC emission color points as a function of the doping concentration of Yb^{3+} , Er^{3+} , and Tm^{3+} is also illustrated in the 1931 Commission Internationale de l'Eclairage (CIE) chromaticity diagram, as shown in Fig. 4. From the measured spectra as shown in Fig. 2, the UC emission colors are significantly changed from blue (Point a in Fig. 4) to green (Point c in Fig. 4) by adjusting the

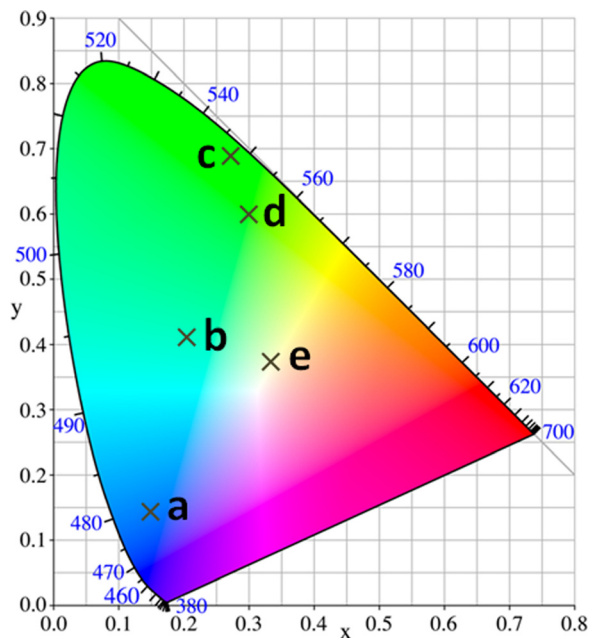


FIG. 4. CIE chromaticity diagrams for $\text{BTO}:\text{Ln}^{3+}$ phosphors under 980 nm laser excitation. (a) $\text{BTO}:\text{2\%Yb}^{3+}, \text{0.2\%Tm}^{3+}$; (b) $\text{BTO}:\text{2\%Yb}^{3+}, \text{0.02\%Er}^{3+}, \text{0.2\%Tm}^{3+}$; (c) $\text{BTO}:\text{2\%Yb}^{3+}, \text{0.1\%Er}^{3+}, \text{0.2\%Tm}^{3+}$; (d) $\text{BTO}:\text{5\%Yb}^{3+}, \text{0.1\%Er}^{3+}, \text{0.2\%Tm}^{3+}$; and (e) $\text{BTO}:\text{5\%Yb}^{3+}, \text{0.02\%Er}^{3+}, \text{0.2\%Tm}^{3+}$.

TABLE I. Chromaticity coordinates (x , y) of the $\text{BTO}:\text{Ln}^{3+}$ phosphors.

Samples	Chromaticity coordinate (x)	Chromaticity coordinate (y)
$\text{BTO}:\text{2\%Yb}, \text{0.2\%Tm}$	0.145	0.140
$\text{BTO}:\text{2\%Yb}, \text{0.02\%Er}, \text{0.2\%Tm}$	0.207	0.411
$\text{BTO}:\text{2\%Yb}, \text{0.1\%Er}, \text{0.2\%Tm}$	0.273	0.685
$\text{BTO}:\text{5\%Yb}, \text{0.1\%Er}, \text{0.2\%Tm}$	0.299	0.592
$\text{BTO}:\text{5\%Yb}, \text{0.2\%Er}, \text{0.2\%Tm}$	0.301	0.630
$\text{BTO}:\text{2.5\%Yb}, \text{0.5\%Er}$	0.329	0.652
$\text{BTO}:\text{5\%Yb}, \text{0.02\%Er}, \text{0.2\%Tm}$	0.328	0.352

concentrations of the activators (Er^{3+} and Tm^{3+}), when the concentration of Yb^{3+} ion is fixed. It is known that Yb^{3+} ion acting as sensitizer has a great influence on the UC emissions. Compared with the UC spectra in Figures 2(b) and 2(c), the blue and red emission intensities are strongly enhanced with increasing Yb^{3+} doping concentration from 2 to 5 mol.%. With the increase of Yb^{3+} ion concentration, it also can be seen that the intensity ratios of the green to the blue and red emission decrease markedly, and the chromaticity coordinate shifts into the green-yellow region (Point d in Fig. 4). Interestingly, a white UC emission is achieved by controlling the relative intensity of RGB in $\text{BTO}:\text{5\%Yb}^{3+}, \text{0.02\%Er}^{3+}, \text{0.2\%Tm}^{3+}$ (Fig. 2(d)). Its chromaticity coordinate falls near to the white region (Point e in Fig. 4).

In the above experiments, we have demonstrated that tunable UC emissions from blue to white in $\text{BTO}:\text{Ln}^{3+}$ powders. As mentioned above, BTO can be considered an important thin-film integrated photonic host. Compared with bulks and powders, the utilization of a thin-film structure facilitates the fabrication and integration of devices.²² Silicon wafers are widely available in semiconductor industry. Perovskite oxides grown on the silicon can be integrated as part of metal-oxide-semiconductor fabrication process.²³ The measured sample consisted a 200-nm-thick ITO electrode and a 600-nm-thick $\text{BTO}:\text{5\%Yb}^{3+}, \text{0.1\%Er}^{3+}, \text{0.2\%Tm}^{3+}$ thin film deposited on Pt-Si substrate. The XRD pattern of as-obtained $\text{BTO}:\text{Yb/Er/Tm}$ thin film on Pt-Si substrate is shown in Fig. 5. The surface of Pt-Si substrate is smooth and

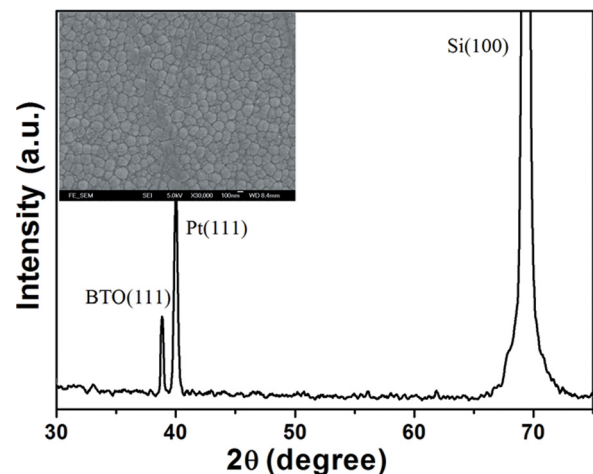


FIG. 5. XRD pattern of $\text{BTO}:\text{Yb/Er/Tm}$ film grown on Pt-Si substrate. The inset shows the FE-SEM image of the film.

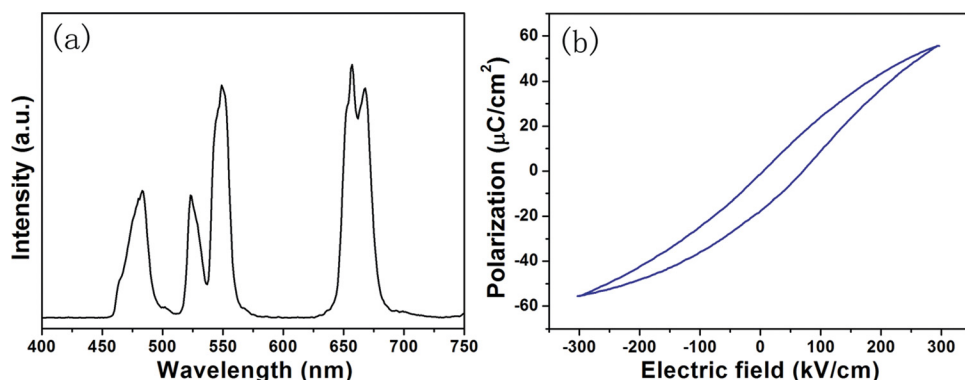


FIG. 6. (a) The UC emission spectrum of BTO:5%Yb³⁺, 0.1%Er³⁺, 0.2%Tm³⁺ thin film grown on Pt-Si substrate. (b) The hysteresis loop of the ferroelectric BTO:Yb/Er/Tm film grown on Pt-Si substrate with ITO top electrode.

flat (not shown here). It is known that Pt-Si can be widely utilized as substrate to fabricate ferroelectric thin films. In the θ - 2θ scan, the BTO (111) peak was observed at 38.8° , while the Pt (111) and Si (100) peaks from Pt/Si wafers are located at 39.9° and 69.1° , respectively. No other peaks were present. This shows that the Yb³⁺/Er³⁺/Tm³⁺ tri-doped BTO thin film is highly oriented grown on Pt-Si substrate. The FE-SEM image illustrates the surface morphology of the as-prepared thin film (inset in Fig. 5). The FE-SEM image confirms that BTO:5%Yb³⁺, 0.1%Er³⁺, 0.2%Tm³⁺ thin film is well-prepared, with a uniform ~ 150 nm grain texture.

Figure 6(a) shows the UC emission spectrum of BTO:5%Yb³⁺, 0.1%Er³⁺, 0.2%Tm³⁺ thin film. It indicates that BTO:Yb/Er/Tm film can also give three typical RGB emission bands. We may predict that multicolor emissions can be achieved by controlling the relative intensity of RGB emissions in the thin-film structure. A well-defined polarization hysteresis loop measured on BTO:Yb/Er/Tm thin film grown on Pt-Si substrate is shown in Fig. 6(b). The remanent polarization ($2P_r$) is determined to be $17.8 \mu\text{C}/\text{cm}^2$. The hysteresis loop is shifted in the positive direction. This imprint effect is probably due to the asymmetric interfacial properties of the top and bottom electrodes to the BTO film.²⁴ The measured hysteresis loop confirms the reservation of ferroelectricity from BTO:Yb/Er/Tm thin-film. The experimental results suggest that the obtained BTO:Yb/Er/Tm thin-film is potentially promising for various applications as a multifunctional material in which luminescent and ferroelectric properties co-exist.

IV. CONCLUSION

In conclusion, we have synthesized Yb³⁺, Er³⁺, and Tm³⁺ tri-doped BTO phosphors with various doping concentrations via solid-state reaction method. By precise control of the dopant concentrations, the UC emission colors can be readily tuned. Yb³⁺ ions as sensitizer have a great influence on the UC emission spectra and color tuning. An optimal white-emitting light with color coordinate ($x=0.328$, $y=0.352$) is achieved by adjusting the relative RGB intensities. Strong UC emission was also observed in lanthanide doped BTO thin films. The obtained luminescent thin film also retains ferroelectric properties. The results in our study demonstrate that the potential of lanthanide-doped BTO as a

multifunctional material for display, solid-state lighting and upconversion luminescence biosensor.

ACKNOWLEDGMENTS

The work described in this paper was supported in part by the National Natural Science Foundation of China (No. 51272218) and Hong Kong Polytechnic University Internal Grant (A-PL50).

- ¹F. Wang, Y. Han, C. S. Lim, Y. H. Lu, J. Wang, J. Xu, H. Y. Chen, C. Zhang, M. H. Hong, and X. G. Liu, *Nature* **463**, 1061 (2010).
- ²S. Schietinger, T. Aichele, H. Q. Wang, T. Nann, and O. Benson, *Nano Lett.* **10**, 134 (2010).
- ³G. Ren, S. Zeng, and J. Hao, *J. Phys. Chem. C* **115**, 20141 (2011).
- ⁴A. Shalav, B. S. Richards, T. Trupke, K. W. Krämer, and H. U. Güdel, *Appl. Phys. Lett.* **86**, 013505 (2005).
- ⁵F. Vetrono, V. Mahalingam, and J. Capobianco, *Chem. Mater.* **21**, 1847 (2009).
- ⁶S. Heer, O. Lehmann, M. Haase, and H. U. Güdel, *Angew. Chem., Int. Ed.* **42**, 3179 (2003).
- ⁷F. Wang and X. G. Liu, *J. Am. Chem. Soc.* **130**, 5642 (2008).
- ⁸G. G. Li, M. Sheng, D. L. Geng, D. M. Yang, C. Peng, Z. Y. Cheng, and J. Lin, *Cryst. Eng. Comm.* **14**, 2100 (2012).
- ⁹S. Sivakumar, F. C. J. M. van Veggel, and M. Raudsepp, *J. Am. Chem. Soc.* **127**, 12464 (2005).
- ¹⁰Z. L. Wang, J. H. Hao, and H. L. W. Chan, *J. Mater. Chem.* **20**, 3178 (2010).
- ¹¹C. M. Zhang, P. A. Ma, C. X. Li, G. G. Li, S. S. Huang, D. M. Yang, M. Sheng, X. J. Kang, and J. Lin, *J. Mater. Chem.* **21**, 717 (2011).
- ¹²H. T. Wong, H. L. W. Chan, and J. H. Hao, *Opt. Express* **18**, 6123 (2010).
- ¹³J. S. Wu, C. L. Jia, K. Urban, J. H. Hao, and X. X. Xi, *J. Mater. Res.* **16**, 3443 (2001).
- ¹⁴S. Y. Chu, C. H. Wen, S. L. Tyan, Y. G. Lin, Y. D. Juang, and C. K. Wen, *J. Appl. Phys.* **96**, 2552 (2004).
- ¹⁵Y. X. Liu, W. A. Pisarski, S. J. Zeng, C. F. Xu, and Q. B. Yang, *Opt. Express* **17**, 9089 (2009).
- ¹⁶G. J. Ding, F. Gao, G. H. Wu, and D. H. Bao, *J. Appl. Phys.* **109**, 123101 (2011).
- ¹⁷D. Y. Wang, S. Li, H. L. W. Chan, and C. L. Choy, *Appl. Phys. Lett.* **96**, 061905 (2010).
- ¹⁸Y. Zhang, J. H. Hao, C. L. Mak, and X. H. Wei, *Opt. Express* **19**, 1824 (2011).
- ¹⁹J. H. Hao, Y. Zhang, and X. H. Wei, *Angew. Chem., Int. Ed.* **50**, 6876 (2011).
- ²⁰C. G. Jiang, L. Fang, M. R. Shen, F. G. Zheng, and X. L. Wu, *Appl. Phys. Lett.* **94**, 071110 (2009).
- ²¹T. C. Huang and W. F. Hsieh, *J. Fluoresc.* **19**, 511 (2009).
- ²²Y. Zhang, G. Y. Gao, H. L. W. Chan, J. Y. Dai, Y. Wang, and J. H. Hao, *Adv. Mater.* **24**, 1729 (2012).
- ²³M. P. Warusawithana, C. Cen, C. R. Slesman, J. C. Woicik, Y. Li, L. F. Kourkoutis, J. A. Klug, H. Li, P. Ryan, L. P. Wang, M. Bedzyk, D. A. Muller, L. Q. Chen, J. Levy, and D. G. Schlom, *Science* **324**, 367 (2009).
- ²⁴K. J. Choi, M. Biegalski, Y. L. Li, A. Sharan, J. Schubert, R. Uecker, P. Reiche, Y. B. Chen, X. Q. Pan, V. Gopalan, L. Q. Chen, D. G. Schlom, and C. B. Eom, *Science* **306**, 1005 (2004).